NEUROIMAGE **8,** 229–239 (1998)
ARTICLE NO. NI980361

Identification of EEG Events in the MR Scanner: The Problem of Pulse Artifact and a Method for Its Subtraction

Philip J. Allen,* Giovanni Polizzi,† Karsten Krakow,† David R. Fish,* and Louis Lemieux†

**Department of Clinical Neurophysiology, The National Hospital for Neurology and Neurosurgery, Queen Square, London, UK; and †The Epilepsy Research Group, Department of Clinical Neurology, Institute of Neurology, and National Society for Epilepsy, Chalfont St. Peter, Buckinghamshire, UK*

Received February 3, 1998

Triggering functional MRI (fMRI) image acquisition immediately after an EEG event can provide information on the location of the event generator. However, EEG artifact associated with pulsatile blood flow in a subject inside the scanner may obscure EEG events. This pulse artifact (PA) has been widely recognized as a significant problem, although its characteristics are unpredictable. We have investigated the amplitude, distribution on the scalp, and frequency of occurrence of this artifact. This showed large interindividual variations in amplitude, although PA is normally largest in the frontal region. In five of six subjects, PA was greater than 50 μV in at least one of the temporal, parasagittal, and central channels analyzed. Therefore, we developed and validated a method for removing PA. This subtracts an averaged PA waveform calculated for each electrode during the previous 10 s. Particular attention has been given to reliable ECG peak detection and ensuring that the average PA waveform is free of other EEG artifacts. Comparison of frequency spectra for EEG recorded outside and inside the scanner, with and without PA subtraction, showed a clear reduction in artifact after PA subtraction for all four frequency ranges analyzed. As further validation, lateralized epileptiform spikes were added to recordings from inside and outside the scanner: PA subtraction significantly increased the proportion of these spikes that were correctly identified and decreased the number of false spike detections. We conclude that in some subjects, EEG/fMRI studies will be feasible only using PA subtraction.

INTRODUCTION

Functional MRI (fMRI) can detect areas of brain activation, and hence fMRI acquisition triggered immediately after an EEG event may help localize the event generators. This has found application in the study of basic EEG features such as alpha rhythm (Patel *et al.*, 1997) and sleep phenomena (Huang-Hellinger *et al.*, 1995) and in epilepsy (Warach *et al.*, 1996). As the peak blood oxygenation level change detected by fMRI occurs approximately 4 to 7 s after the EEG event (Hennig *et al.*, 1995), the EEG event must be identified rapidly and hence high quality EEG in the scanner is essential for these experiments. Unfortunately, interactions between the patient, EEG electrodes leads, and the magnetic fields in the scanner may result in artifacts which obscure the EEG.

There are two physical principles which underlie the generation of these artifacts. First, if the magnetic flux through a loop changes, an electromotive force (emf) is induced in the loop (Faraday's induction law). Second, there is a blood flow effect, whereby the movement of blood (a conductor) normal to a magnetic field leads to induced potentials (Kolin, 1952; Tenforde *et al.*, 1983).

The former principle may result in artifact as follows: (a) outside the magnet bore, the static field (B_0) becomes nonuniform and hence a moving interelectrode lead loop may experience a change in flux resulting in an induced emf; (b) the switching magnetic fields applied during image acquisition may induce emfs in the electrode leads and head, independent of head or lead movement and tilting; (c) movement of the subject's head and hence the attached electrode leads may change the area of interelectrode lead loops normal to B_0, resulting in an induced emf in the leads; and (d) head tilting may change the area of scalp normal to B_0, resulting in an emf induced on the scalp.

By twisting electrode leads together from the patient's head to the amplifier inputs and securely fixing the leads to a stationary surface, factor (a) (nonuniform field) can be minimized. Artifacts due to factor (b) (image acquisition) are transient and occur after the EEG event used to trigger fMRI. Artifacts due to factors (c) and (d) (electrode lead/head movement) result from patient movement. Gross movement (for example head turning, talking) causes large artifacts, although recording from a movement detector may help identify these (Hill *et al.*, 1995) and providing that patient movement is minimal, a prerequisite of fMRI, only a short duration of the EEG recording is affected. However, small pulse-related body movements may produce pulse artifact (PA). Ives has suggested that these movements

1053-8119/98 $25.00

may result from the acceleration and abrupt directional change in blood flow in the aortic arch during each heart beat (Ives *et al.*, 1993). Scalp movement may also occur due to the expansion and contraction of scalp arteries. PA is a more significant problem: it may affect EEG recorded from a wide area of the scalp and have a large amplitude peak followed by a complex waveform persisting throughout the interpulse period, obscuring EEG features in a large proportion of a recording (Felblinger *et al.*, 1997). The amplitude of this artifact is proportional to B_0 and the rate of change in area normal to B_0 of interelectrode leads loops and the scalp due to pulse-related head movement. Minimizing PA by preventing these small head movements for the duration of an EEG/fMRI study (which may last over an hour) is impractical.

The blood flow effect may also result in PA due to the electric field associated with the pulsatile movement of blood perpendicular to B_0. This phenomenon is well known in electrocardiogram monitoring and results in an augmented T-Wave (Wendt *et al.*, 1988). The amplitude of the artifact is proportional to B_0, blood flow, the orientation of flow with respect to B_0, and the proximity of the EEG electrodes to blood vessels. Hence, minimizing this artifact is difficult: B_0 and blood flow are fixed, there is limited scope for adjusting the position of the subject's head in the scanner and placing electrodes distant from blood vessels is impractical due to the broad coverage of scalp arteries.

Many reports of EEG/fMRI from different centres, using a variety of EEG recording methods, have mentioned this problem (Ives *et al.*, 1993; Hill *et al.*, 1995; Huang-Hellinger *et al.*, 1995; Felblinger *et al.*, 1997), although its amplitude, frequency of occurrence, and distribution on the scalp have not been investigated systematically. Our preliminary EEG/fMRI experiments have, in agreement with these studies, found large interindividual variability in PA amplitude, and this has made the successful execution of EEG/fMRI studies difficult to predict. Hence, it would seem that signal processing techniques to reduce PA would be useful in cases where it obscures the EEG event of interest.

The aims of this study were (1) to measure the amplitude, distribution on the scalp, and frequency of occurrence of PA and (2) if PA appears to restrict the general utility of EEG/fMRI studies, then to develop a method for PA subtraction.

EXPERIMENT 1: THE AMPLITUDE AND DISTRIBUTION OF PULSE ARTIFACT

Materials and Methods

Subjects

This experiment (and Experiment 2) had the approval of the local ethical committee of The National Hospital for Neurology and Neurosurgery and all subjects gave informed consent. EEG was recorded both inside and outside the scanner, from six normal subjects (three male, three female, median age 28.5, range 24 to 33 years).

Methods

This experiment (and Experiment 2) was performed using a 1.5-T Horizon Echospeed MRI scanner (General Electric, Milwaukee, WI). All 19 electrodes in the 10/20 system were recorded (reference Pz) as this allowed the amplitude of PA to be measured over the whole scalp, and wide coverage may be necessary to ensure fMRI acquisitions are triggered on specific stereotyped events (e.g., in a patient with multiple types of focal epileptiform spikes). Ag/AgCl disk electrodes were applied using collodion. These had a 15-kOhm current limiting resistor fitted adjacent to each electrode as an essential part of our patient safety protocol for EEG recording in the MR scanner. This value of resistance is appropriate for the specific scanner and B_0 used in these experiments: a detailed description of the calculation of the safety resistor value is given in Lemieux *et al.* (1997).

Reducing the number and area of interelectrode lead loops by aligning the leads from a chain of electrodes should reduce the PA due to lead movement, and our preliminary recordings have shown that using strips of electrodes with the leads twisted together from the electrodes to the amplifier inputs reduces the PA considerably. Hence, electrode leads were grouped as follows: temporal chains (Fp1, F7, T3, T5, O1 and Fp2, F8, T4, T6, O2) were covered by two strips of five electrodes (electrode spacing 5.5 cm, corresponding to a head circumference of 55 cm), with the electrode shafts aligned in the direction anterior to posterior, and the overlapping parts of the leads twisted together. Electrode positions F3, C3, P3; F4, C4, P4; and Fz, Cz, Pz were covered using three strips of three electrodes with 5.5-cm spacing. The electrode leads from the five strips were brought together at the left side of the subject's neck and connected to the headbox via 2.5-m multicore cables, taped along the side of the movable table under the subject's left side. The EEG leads were brought out of the front of the scanner to avoid restricting the removal of the patient from the scanner.

The nonferrous headbox was placed at the entrance to the bore of the magnet and was connected via a 2-m ribbon cable to a Neurolink Patient Module (Physiometrix, MA) which amplifies and digitizes EEG and transmits it out of the scanner room via a fiber optic to a Neurolink Monitor Module which reconstructs the analog EEG signals. These are then recorded using a digital EEG recording system (overall bandwidth 0.12 to 50 Hz). The Neurolink System reference electrode (connected to Pz in these experiments) is a driven

ground, derived from the average of the EEG signals with respect to amplifier ground, although all the PA measurements were made using digitally remontaged EEG, thereby subtracting the reference.

A minimum of 1 min of EEG, containing periods of eyes open and closed was recorded with the subject supine on the movable scanner table just outside the scanner to confirm that the EEG equipment was functioning correctly and to check that there was no PA outside the scanner. The subject was then advanced into the scanner and recorded for at least 1 min with eyes open and closed. The amplitude of PA, defined as the largest peak to trough deflection, was measured in 13 bipolar channels (giving broad coverage of the scalp), for the first 10 consecutive PA waveforms during eyes closed with no other EEG artifact present. Although a precordial ECG signal might help to identify the precise location of the peak PA, this was not recorded to be certain that no PA was added to the scalp signals due to currents induced in the large interelectrode lead loops between the chest and scalp electrodes.

To confirm that PA is reduced by using strips of electrodes with leads twisted together, PA was also measured from the same electrodes, but with the wires over the scalp untwisted. Some EEG events can be identified with a small number of electrodes (for example alpha rhythm, sleep phenomena) and in theory this may give less PA than for the full 10/20 system, as there are fewer interelectrode lead loops. Hence, to measure PA under optimal conditions with minimum interelectrode loops (<2 cm^2) we also recorded from individual pairs of electrodes from the same strip as follows: Fp1–F7 with reference at T3, T3–T5 with reference at O1, T5–O1 with reference at T3, F3–C3 with reference at P3 (and the contralateral channels), and Fz–Cz with reference at Pz.

Results

The mean amplitudes of PA over all six recordings (78 channels in total) was 58 μV (SD = 58 μV) for the untwisted electrode leads and 36 μV (SD = 34 μV) for the electrodes with leads twisted together, which was significantly different ($P < 0.001$, two-tailed paired t test). This represents a reduction in PA amplitude (relative to the PA for untwisted leads) of 38%.

Comparison of the PA from identical bipolar channels recorded from single pairs of electrodes (minimal possible interelectrode loop area) and from the full 10/20 system (with leads twisted together) did not show a significant difference ($P = 0.45$, two-tailed paired t test) and the mean amplitude of PA over all six recordings (54 channels in total) was 38 μV (SD = 36 μV) for the single pairs and 36 μV (SD = 36 μV) for the full 10/20 system, indicating that recording from single pairs of electrodes did not consistently reduce PA in comparison to recording from the full 10/20 system.

For the recordings from the full 10/20 system with the leads twisted together, PA was consistently largest in channels with frontal-polar or fronto-central electrodes and showed large intra- and interindividual variations in amplitude (Fig. 1). In five of six of these recordings, PA was >50 μV in at least one channel. Excluding channels with fronto-polar and frontal electrodes (Fp1, Fp2, F4, F3, and Fz), PA was <50 μV in all the remaining channels in only three of six subjects. The amplitude of most scalp EEG events is normally between 10 and 150 μV.

EXPERIMENT 2: PULSE ARTIFACT SUBTRACTION

Materials and Methods

The Subtraction Algorithm

The subtraction algorithm is applied on a second-by-second basis as follows (see Fig. 2): ECG peaks (QRS complexes) in the previous 10 s are identified (Fig. 2A). The average PA waveform for the period ± half the R–R interval, time-locked to the ECG peaks in this period, is then calculated for each referential EEG signal (Fig. 2B). This average waveform is then subtracted at the times corresponding to the ECG peaks identified during the penultimate second of EEG and the 1-s periods bracketing this (Fig. 2C). The penultimate second of corrected EEG data is then displayed. The penultimate rather than the last second in the 10-s period is displayed, as ECG peaks occurring up to half an R–R interval after the second displayed will have a component of the averaged PA waveform which requires subtracting from the EEG in that second. Hence, the algorithm delays the display of EEG by at least 1 s. A 10-s averaging period was chosen as a compromise between being long enough to separate the PA from the underlying EEG by averaging out the cerebrally generated components and being short enough to adapt to changes in the PA waveform.

It is important to detect a high proportion of ECG peaks, as an occasional missed peak results in the isolated appearance of PA which may be falsely interpreted. However, the ECG signal may also contain artifacts due to the same reasons that cause PA in the EEG. Hence considerable effort has been directed at producing a robust peak detection method which operates as follows. ECG peaks in the current 10-s period are initially identified by searching for a turning point following an amplitude threshold crossing. To assist in setting an appropriate threshold, a three-coefficient moving average low-pass filter is applied to the ECG channel to reduce high-frequency noise, and a 25-coefficient finite impulse response high-pass filter (cut-off 20 Hz) is applied to attenuate baseline changes. To reduce false ECG peak detection due to artifact in the ECG channel, the 10-s period is divided into half-

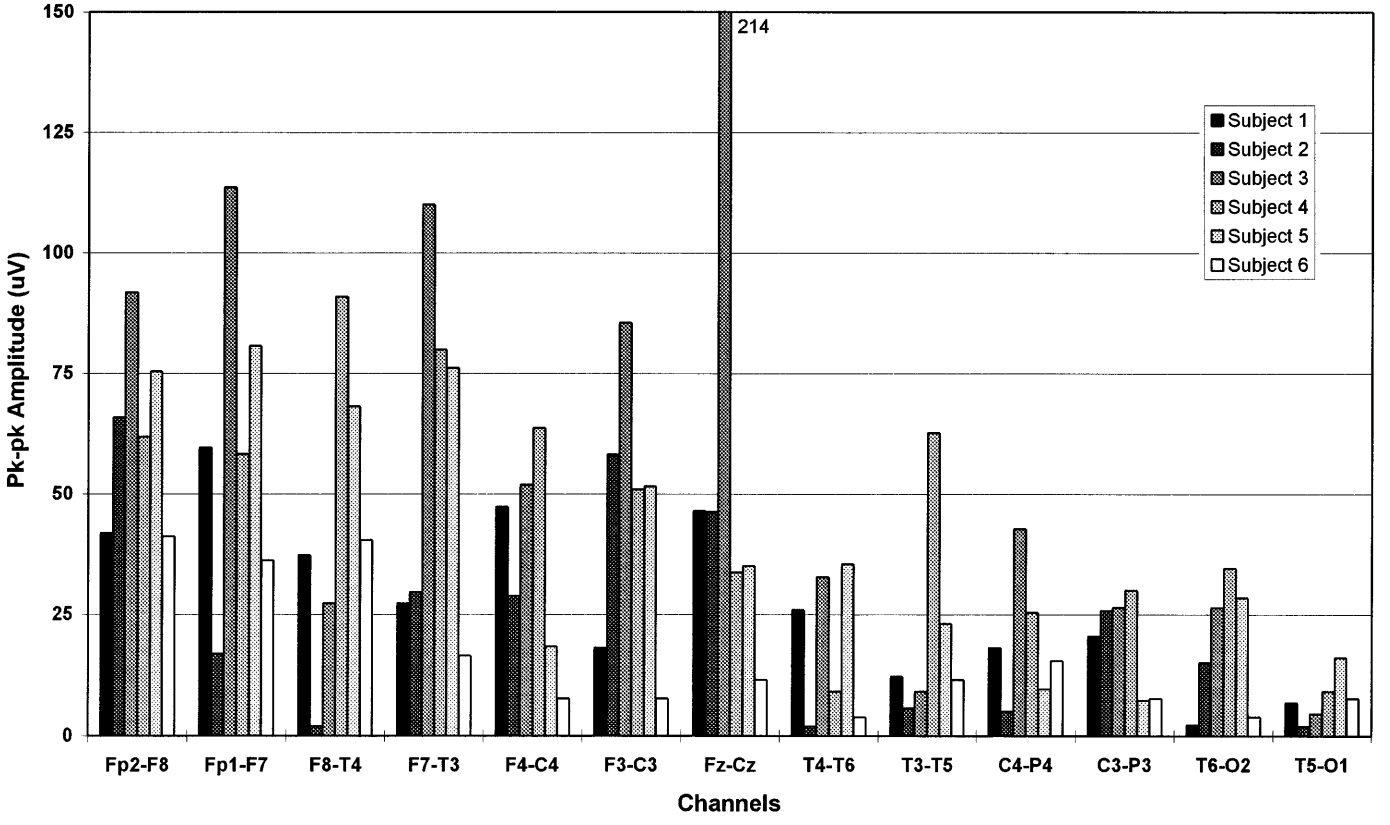

FIG. 1. Distribution of pulse artifact on the scalp for the six normal subjects recorded inside the scanner with the full 10/20 system of electrodes, with electrode leads twisted together. Each bar represents the mean peak-to-peak amplitude of 10 consecutive PA waveforms. The artifact is greatest in channels with a frontal polar or fronto-central electrode and shows large interindividual variation in amplitude.

second sections, and the mean magnitude of signal calculated for each section. Any section with magnitude 4 times greater than the mean of the 10 lowest magnitude sections is rejected as being likely to contain artifact. The amplitude threshold is then set at the mean amplitude plus or minus 33% of $|\max - \min|$ in the 10-s period, depending on whether $|\max - \text{mean}|$ exceeds $|\min - \text{mean}|$. The maximum and minimum values are calculated as the mean of the 5 largest and smallest signal values in different half-second sections in the 10-s period (although any of these 5 that are >2 times the smallest are excluded as these are normally large noise spikes which are too brief to affect the mean magnitude of a half-second). ECG peaks are then derived by identifying turning points in the ECG channel following threshold crossings.

To confirm the validity of these ECG peaks, the cross-correlation function is then calculated (for lag range $\pm$ 60 ms) between the ECG waveform at each peak and an averaged ECG waveform. To calculate the latter, the algorithm searches for four successive ECG peaks with R–R interval between 0.5 and 1.5 s and inter-R–R interval variation $<$20% (as these are likely to be QRS complexes, rather than artifact), and the ECG waveform $\pm$0.25 s at these four peaks is then averaged (Fig. 2D). This averaged ECG waveform is then cross-correlated with the waveforms at all the ECG peaks and peaks with a cross-correlation $<$0.65 rejected (Fig. 2E). Finally, to check if any QRS complexes have been missed, the intervals between ECG peaks are examined for intervals an integer ($>$1) number of the mean R–R interval, and new ECG peaks added accordingly (Fig. 2F).

To calculate the average PA in each EEG channel, the sections of EEG signal $\pm$ half the mean R–R interval centered on the ECG peaks plus a time delay are averaged (Fig. 2G). The time delay (0.21 s[1]) is required as the PA peak in an EEG channel normally occurs after the QRS complex. Before including sections of EEG in the average, each section is tested for artifacts which would corrupt the average PA waveform. EEG sections with mean magnitude $>$3 times that for the

[1] The value 0.21 s was derived from the median interval between a QRS complex and a PA peak measured in seven subjects (five measures per subject selected to represent the widest range of R–R interval in these recordings). The median delay was 0.21, range 0.15 to 0.24 s, and the median R–R interval 0.98, range 0.74 to 1.54 s. This delay is relatively constant for each subject (maximum range 0.04 s), irrespective of R–R interval variation.

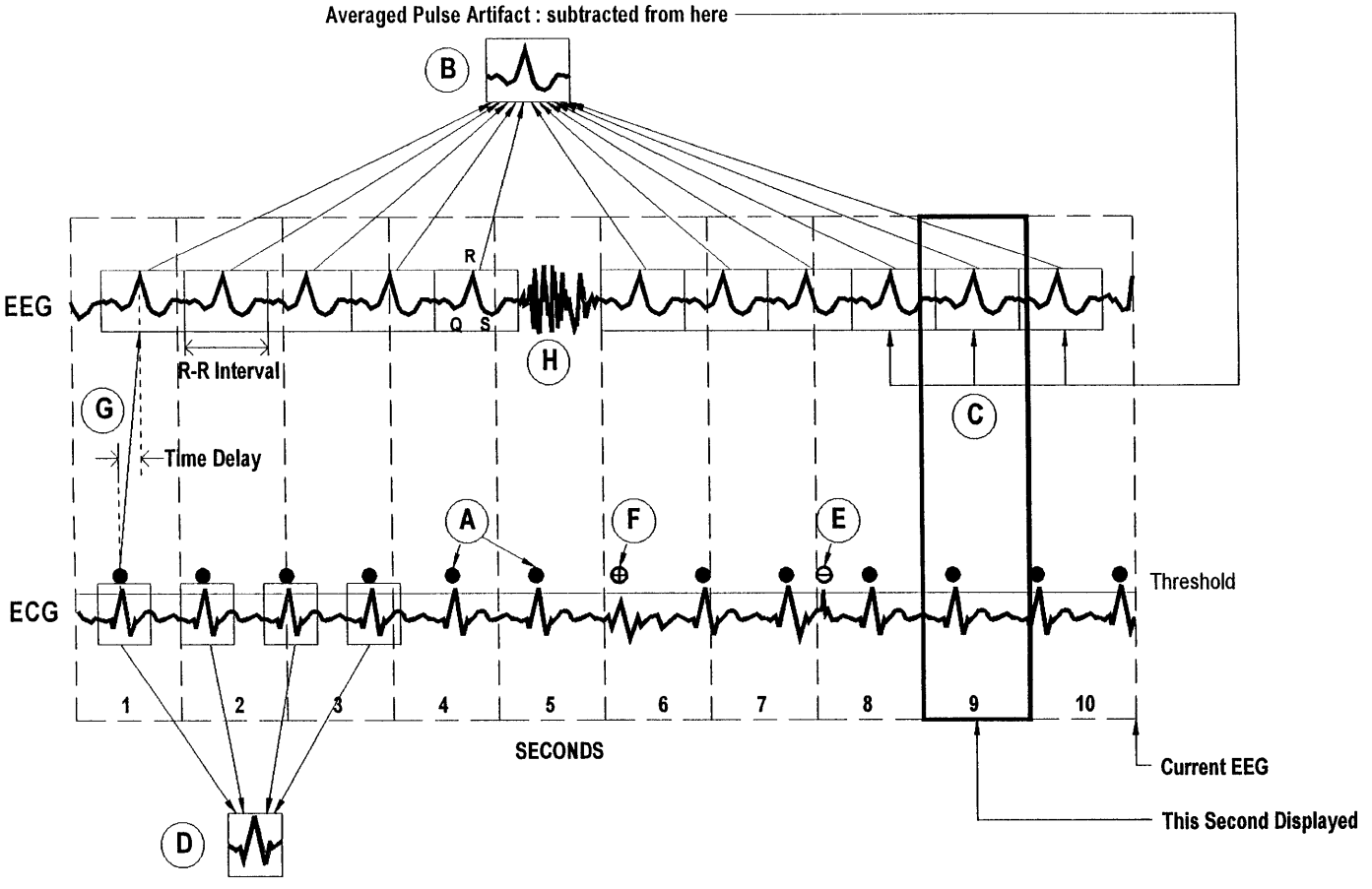

FIG. 2. This shows a schematic of the PA subtraction method. This method processes EEG on a second-by-second basis and requires the previous 10 s of EEG and ECG signals. (A) An ECG peak corresponding to a QRS complex is identified by detection of a turning point following an amplitude threshold crossing. (B) PA waveforms in the EEG channels, time-locked to the ECG peaks (for example at points A and F) are averaged. (C) The averaged PA signal for each channel is subtracted from the EEG signals at times corresponding to the ECG peaks (plus the time interval described in part G below) in the last 3 s). This ensures all PA waveforms affecting the penultimate second of EEG are subtracted: this second of EEG is then displayed. (D) To confirm that an ECG peak detection corresponds to a QRS complex, an averaged QRS waveform is calculated from the first four ECG peak detections with temporal characteristics which indicate a high probability of being QRS complexes. This is then cross-correlated with the ECG waveform at each peak detection. (E) ECG peaks corresponding to noise in the ECG signal are rejected due to a low value of cross-correlation with the averaged QRS waveform calculated in D. (F) QRS complexes which are not detected by threshold crossing are identified by detecting an "R–R" interval between successive ECG peaks which is an integer number of the mean R–R interval and extra ECG peaks are added accordingly. (G) The sections of EEG (duration ± half the mean R–R interval) occurring a short time interval after the ECG peaks are averaged. A time interval is necessary as the peak of the PA in an EEG channel normally occurs a short time after the QRS complex. (H) If the section of EEG time locked to an ECG peak contains other artifacts, the section is excluded from the average PA waveform.

minimum section are excluded as these are likely to contain artifact such as eye blinks or muscle (Fig. 2H). In addition, our results for measuring the amplitude of PA showed a worst case amplitude of 175 μV. Hence, any section containing a sample greater than two times this is also excluded as this is unlikely to be PA. If fewer than two EEG sections in the current 10-s period are artifact free (for example because of persistent movement artifact or frequent spikes), the previous averaged PA waveform is used instead. Finally, although averaging helps reject non-PA EEG activity from the waveform to be subtracted, slow baseline trends such as the exponential return to baseline after a large artifact are poorly rejected by averaging. To remove these, a first order polynomial calculated by linear regression is fitted to each section of EEG and subtracted before averaging. The average PA waveform is then subtracted from the referential EEG signals at the times synchronized to the ECG peaks. The corrected 1-s section of EEG is then displayed.

Subjects

PA subtraction was tested on the nine recordings performed to date inside the scanner in which ≥10 electrodes were recorded, PA exceeded 50 μV in >2

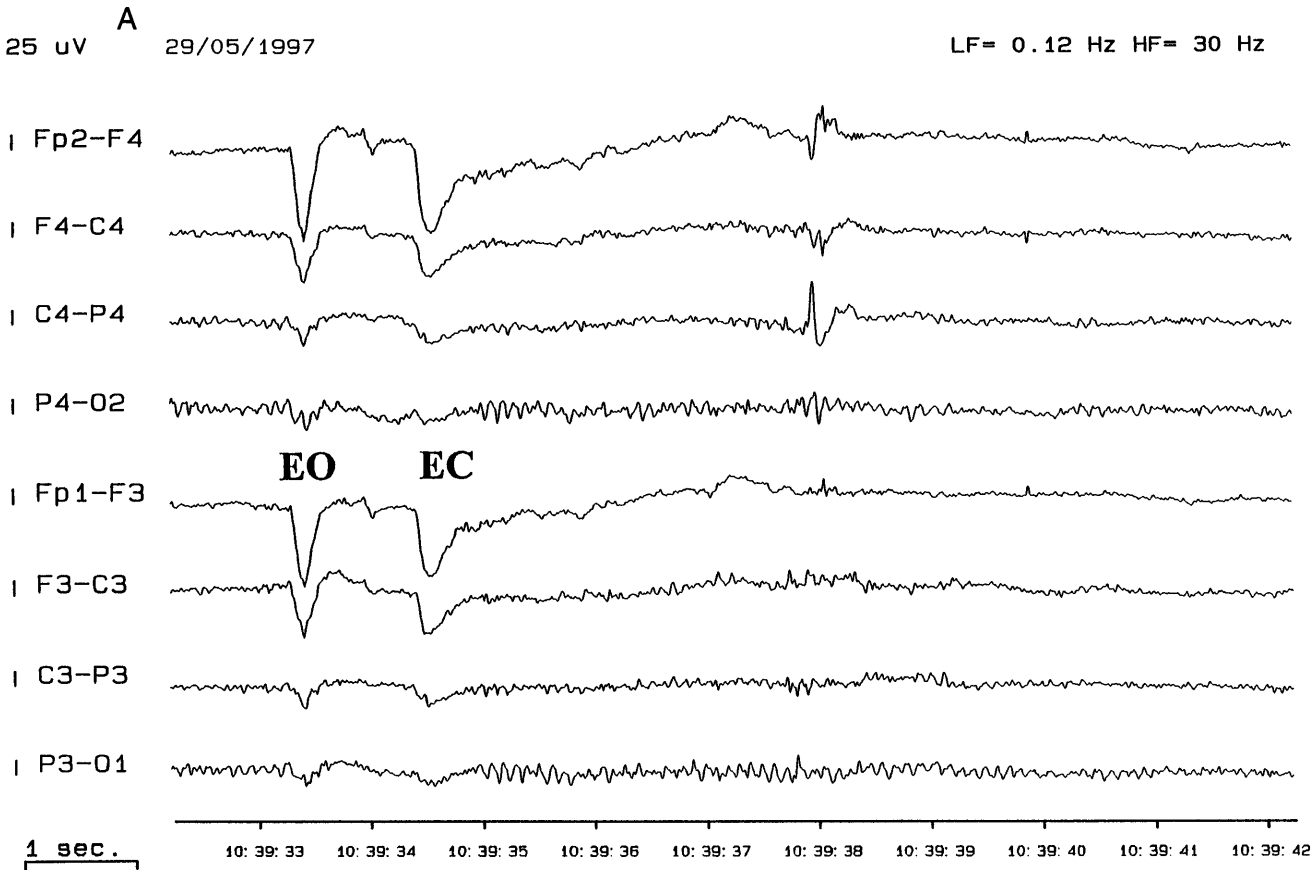

FIG. 3. (A) EEG recording from a normal subject outside the scanner. A lateralized spike with maximum potential at F4 has been added to this record at 10:39:38. (B) The same subject inside the scanner. Large amplitude PA is widespread with peak amplitude approximately synchronous with the *t* wave in the ECG channel. A similar spike (to that in 3A) has been added to this record at 15:13:42, but this is now difficult to identify. (C) The section of EEG illustrated in B, but with PA subtraction applied. The spike is now clearly visible. Alpha rhythm in channels P4–O2 and P3–O1 is also more clearly visible than in 3B and of similar amplitude, frequency, and distribution to that outside the scanner.

bipolar channels formed from adjacent 10/20 system electrodes, and either a precordial ECG channel was recorded (six recordings) or an electrode pair on the scalp had PA with a clearly defined large amplitude peak which could be used reliably for "ECG" peak detection (three recordings). These nine recordings were made from nine subjects: eight normal volunteers and one patient with generalized spike-and-wave (one female, eight male, median age 29, range 24 to 41 years).

Validation: Frequency Analysis

To test the effectiveness of the subtraction algorithm, frequency spectra were calculated for bipolar EEG signals from outside the scanner, inside, and the same period inside with PA subtraction. Frequency spectra were used instead of measuring the peak-to-peak PA amplitude (as for Experiment 1), as it was normally difficult to discern a peak in the waveform after PA subtraction. The EEG recording equipment was as described in Experiment 1. ECG signals were recorded from pregelled Ag/AgCl electrodes applied to the left side of the chest, spaced approximately 10 cm apart and connected to the auxiliary channels of the Neurolink Patient Module. Current-limiting resistors (75 kOhm) were fitted to each of these leads adjacent to the electrodes. In these recordings, averaged spectra were calculated for 41 s of EEG (256 sample nonoverlapped epochs, Hanning windowed) with eyes closed and no other EEG artifacts present, for eight bipolar channels formed from adjacent 10/20 system electrodes. All subjects were in a relaxed state both inside and outside the scanner. The mean amplitude of signal in frequency bands 0.8 to 4, 4 to 8, 8 to 12, and 12 to 24 Hz were then determined for each channel, and the percentage difference between the mean amplitudes outside and inside, with and without PA subtraction, were calculated with respect to the amplitude outside the scanner. These frequency bands were chosen to allow a detailed assessment of the effect of PA subtraction over the frequency range of most EEG activity.

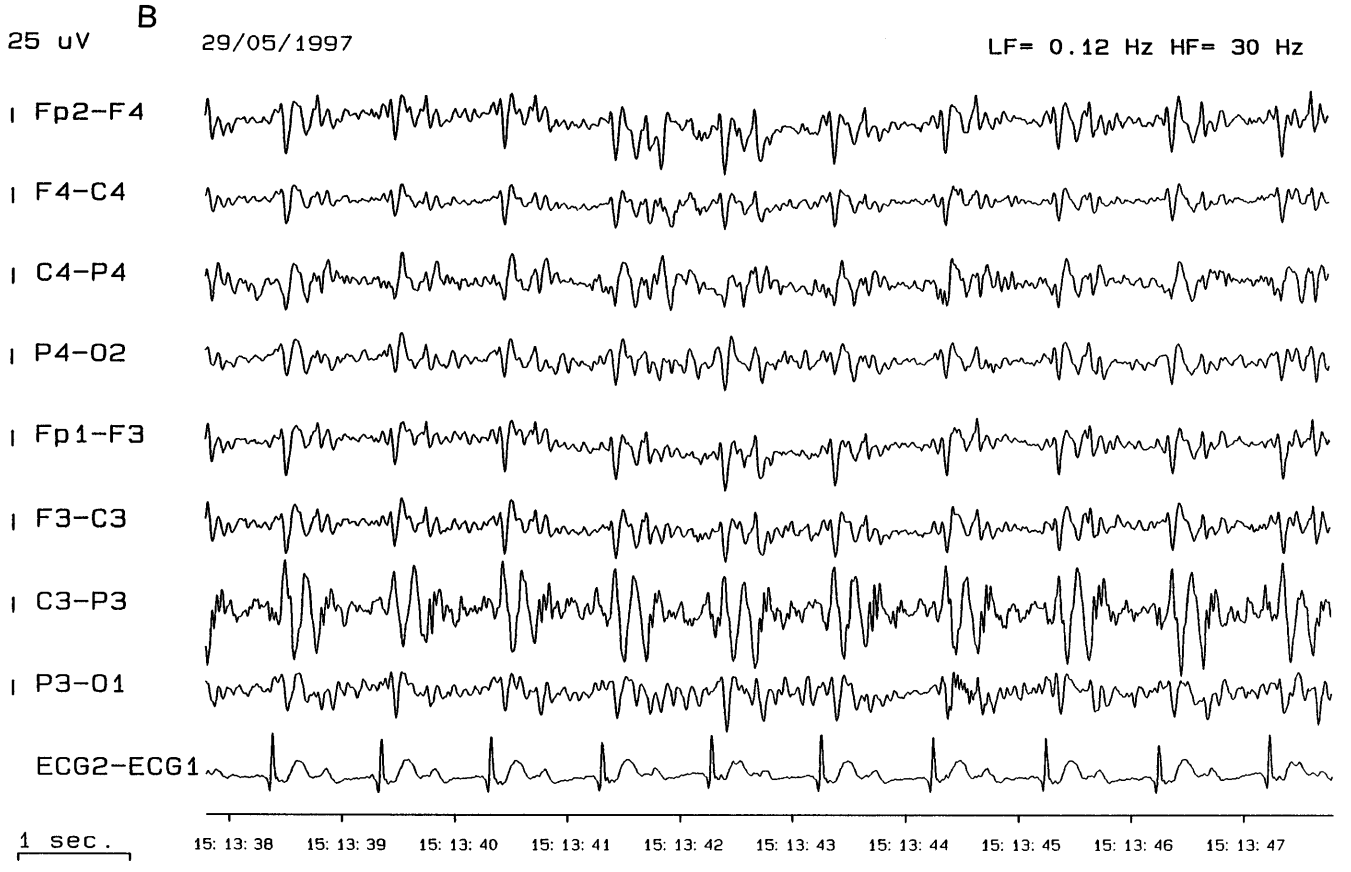
B
25 uV
29/05/1997
LF= 0.12 Hz HF= 30 Hz
Fp2-F4
F4-C4
C4-P4
P4-O2
Fp1-F3
F3-C3
C3-P3
P3-O1
ECG2-ECG1
1 sec.
15: 13: 38
15: 13: 39
15: 13: 40
15: 13: 41
15: 13: 42
15: 13: 43
15: 13: 44
15: 13: 45
15: 13: 46
15: 13: 47

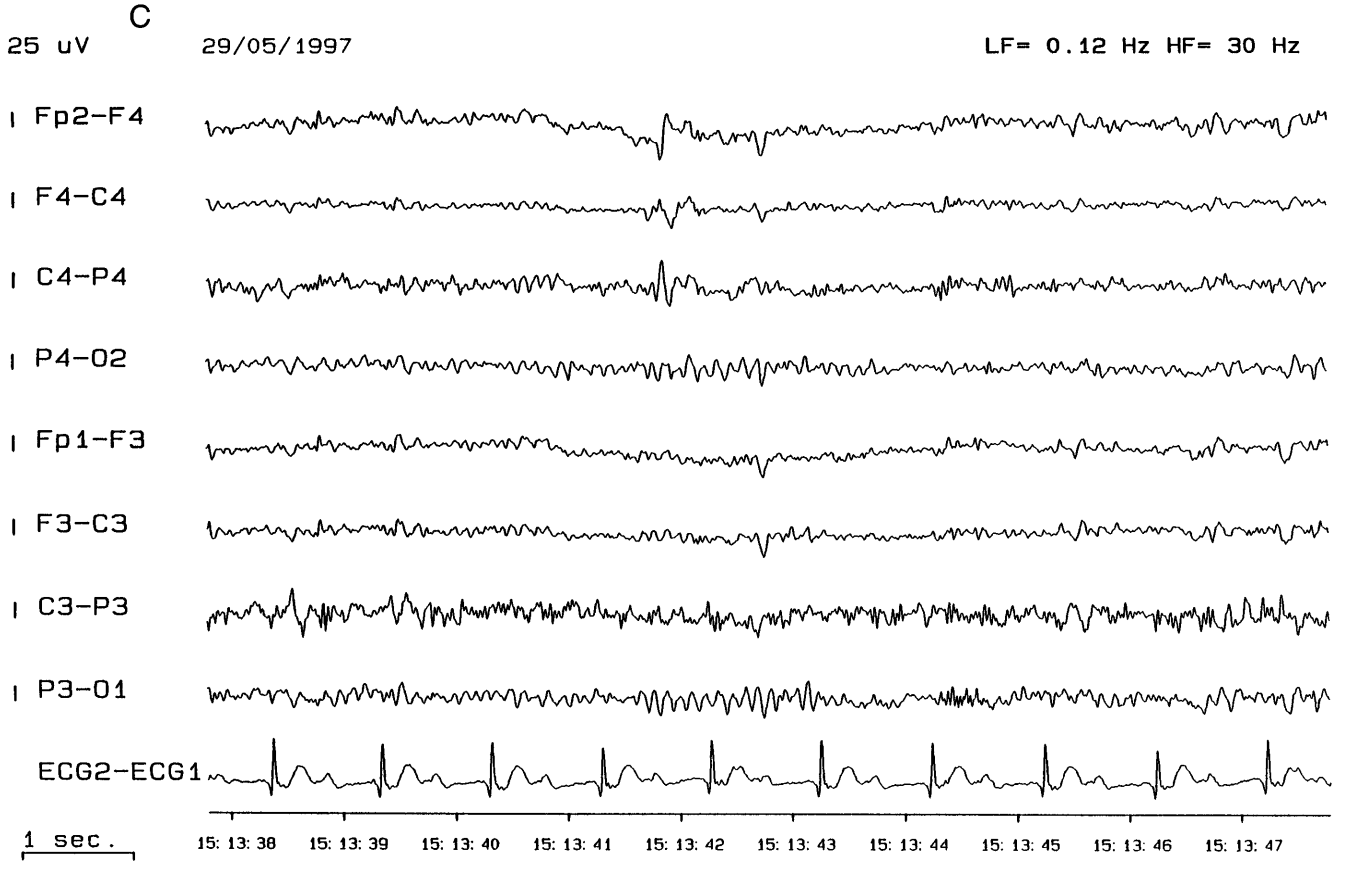
C
25 uV
29/05/1997
LF= 0.12 Hz HF= 30 Hz
Fp2-F4
F4-C4
C4-P4
P4-O2
Fp1-F3
F3-C3
C3-P3
P3-O1
ECG2-ECG1
1 sec.
15: 13: 38
15: 13: 39
15: 13: 40
15: 13: 41
15: 13: 42
15: 13: 43
15: 13: 44
15: 13: 45
15: 13: 46
15: 13: 47

Validation: Identification of EEG Spikes

Although spectral analysis provides a useful quantitative measure of the effectiveness of PA subtraction, this is based on averaged measures and does not directly indicate whether PA subtraction assists the identification of EEG events. Hence, to provide a more realistic assessment of the method, lateralized EEG spikes were digitally added at random times to the nine recordings, and the number of correctly identified spikes and false spike detections with and without PA subtraction measured (Fig. 3). Adding lateralized spikes to recordings known to be otherwise free of these events enabled us to determine unambiguously the accuracy of spike identification. Lateralized spikes were selected as the EEG event as the purpose of PA subtraction is to help reveal EEG events with amplitude and temporal characteristics that make them likely to be obscured by PA and spikes are of significant interest for EEG/fMRI studies. The criteria for selecting these recordings were the same as for spectral analysis (for the patient with epilepsy, spikes were added to a section of EEG with no generalized spike-and-wave, and this patient did not have lateralized spikes).

All of the nine recordings contained typical EEG artifacts (e.g., movement, eyeblinks, muscle) and the total duration analyzed was 31 min (range 1.5 to 4.9 min per patient) outside the scanner and 34 min (range 2.1 to 4.6 min per patient) inside the scanner. Twenty spikes were added to each of the recordings and these spikes were selected at random from a pool of 10 1-second sections of EEG containing a lateralized spike extracted from a recording of a patient with temporal lobe epilepsy. The spikes were recorded from Fp2, F8, T4, T6, and O2 relative to Pz and were maximal at F8 (median amplitude 68μV, range 54 to 134 μV, bipolar display) but also apparent in Fp2, T4, and T6. The 1-s sections of EEG were added to five EEG electrodes forming a unilateral chain. The EEG sections were tapered by a raised cosine function to reduce discontinuities.

Two experienced EEGers subsequently reviewed each of the recordings, which were presented scrolling at real-time on a computer screen. To simulate an EEG/fMRI experiment in which EEG events should be identified within 4 s in order to acquire images during the peak blood oxygenation response, the EEGers were only presented with the most recent 3 s of EEG for the recordings outside and inside without PA subtraction (this would allow some additional time for manually triggering the scanner). For the recordings inside with PA subtraction, this was reduced to 2 s, as in this case the implementation of the algorithm delays the EEG by 1 s. Each recording was reviewed as follows. First, the EEGers were shown examples of the spikes added to the recording (equivalent to reviewing a patient's EEG before an EEG/fMRI study). The EEGers were then asked to identify spikes added to the recordings from outside the scanner, to measure the EEGer's spike detecting sensitivity. They then identified spikes in the recordings from inside the scanner with, and then without, PA subtraction. This ensured that any improvement in spike identification with PA subtraction was not due to the EEGer becoming more skilled at recognizing spikes in a particular record due to repeated viewing. For each recording, the proportion of spikes correctly identified by each EEGer in the EEG recorded outside the scanner was calculated (P_{Outside}) to reflect the spike detecting sensitivity of the EEGer in the absence of PA. P_{Outside} was then used to weight the proportion of spikes identified in the EEG recorded inside the scanner, with and without PA subtraction, as follows: Proportion of correctly identified spikes = Number of correctly identified spikes/(P_{Outside} × Number of spikes added). The mean percentage (for the two EEGers) of correctly identified spikes and the number of false detections per hour were then calculated for each recording.

Results

Frequency Analysis

The frequency spectra for EEG recorded inside the scanner with no PA subtraction showed a large increase in activity relative to that recorded outside the scanner, in each frequency band analyzed, with the greatest median increase (307%) present in the 4- to 8-Hz range and the smallest increase (90%) in the 12- to 24-Hz band (Fig. 4). PA subtraction reduced this increase significantly in all four frequency bands ($P < 0.001$ two-tailed paired t test for 72 measurements = 8 channels per 9 subjects), with the reduction in median increase as follows: 0.8 to 4 Hz = 119% (no PA subtraction) to 35% (PA subtraction), 4 to 8 Hz = 307 to 78%, 8 to 12 Hz = 160 to 19%, and 12 to 24 Hz = 90 to 25%. PA subtraction reduced the increase in activity inside the scanner in almost all measurements: in 72/72 in the 0.8- to 4-Hz, 4- to 8-Hz, and 12- to 24-Hz bands, and 70/72 in the 8- to 12-Hz band. However, even with PA subtraction, there remained a significant difference between the EEG activity inside and outside the scanner ($P < 0.001$ for each frequency band, two-tailed paired t test for 72 measurements).

Identification of EEG Spikes

The proportion of spikes correctly identified by each EEGer was greater with PA subtraction than without in all nine recordings inside the scanner. The mean proportion of correctly identified spikes outside the scanner was 0.89 (SD = 0.09). The weighted proportion of correctly identified spikes inside the scanner without subtraction was 0.35 (SD = 0.16) and with subtraction 0.73 (SD = 0.16). Comparison of the proportions of

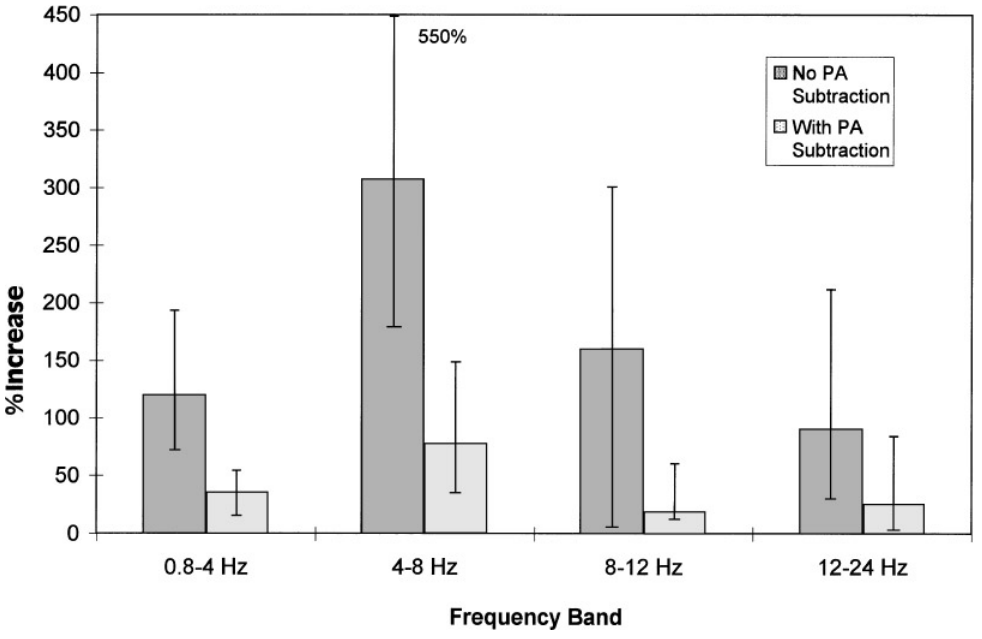

FIG. 4. This shows the median increase (for all nine subjects and eight channels) in EEG amplitude inside the scanner, with and without PA subtraction, for each frequency range. The amplitude is calculated from spectral analysis of 41 s of background EEG: the percentage increase is relative to the amplitude outside the scanner. The error bars show the interquartile ranges.

correctly identified spikes with and without PA subtraction showed a significant difference ($P < 0.001$ two-tailed paired t test). The mean false detection rates per hour of EEG (for the two EEGers) were as follows: Outside = 3.9, Inside without subtraction = 15.7, and Inside with subtraction = 8.7, indicating that although there were more false detections inside than outside the scanner, PA subtraction reduced the number by approximately 45%.

DISCUSSION

Measurement of Pulse Artifact

In agreement with other studies, we found PA to be unpredictable with large interindividual variations in amplitude. Using strips of electrode with twisted leads reduced the amplitude of PA significantly relative to the PA for untwisted leads. This may be due to the potentially large reduction in the number and area of interelectrode lead loops given by the former, and the corresponding reduction of induced emfs in the leads due to pulse-related movement. However, recording from single pairs of electrodes (with minimum possible interelectrode loop) did not give a further reduction in artifact. This suggests that although minimizing large loops can reduce PA, there remains a baseline artifact which is induced on the scalp rather than in the electrode lead loops. Hence, refinement of the arrangement of electrode leads is unlikely to give further reduction in PA.

We have presented here only quantitative PA measures for bipolar as opposed to common reference channels, as the former tend to have lower amplitude PA and are appropriate for detection of most EEG events. Qualitatively, PA in common reference channels was much larger, although this was strongly dependent on the reference electrode used. The reason for PA in frontal channels having larger amplitude remains unclear. It may be that the pulse-related head movement is greater at the front of the head as opposed to the rear which rests on the scanner table. However, there were marked intraindividual asymmetries in PA between contralateral channels, for example F4–C4 greater than F3–C3 but T4–T6 less than T3–T5. This suggests that head movement may be less important than the blood flow effect, since the former is more likely to have a widespread effect, whereas the latter, particularly due to the scalp arteries, is more localized. Scalp arteries are more likely to make a greater contribution than cerebral arteries as the field from the latter will be attenuated significantly by the skull. However, although the relative contributions to PA of head movement and blood flow effect remains unclear, eliminating either is difficult. Hence, we conclude that with the exception of large amplitude (>200 μV) frontal EEG events or lower amplitude events in the posterior/temporal regions, identification of EEG events in many subjects will be extremely difficult unless PA subtraction is used. Furthermore, the amplitude of PA was measured for a B_0 of 1.5 T. A higher B_0 is advantageous

for fMRI and scanners of 3T and 4T are now in use for these studies (Humberstone *et al.*, 1997). As the amplitude of PA is directly related to B_0, the problem of PA is likely to increase for such systems.

Subtraction of Pulse Artifact

The spectral analysis results showed a large increase in EEG amplitude inside the scanner relative to the activity recorded outside in all four frequency ranges analyzed (greatest in the 4- to 8-Hz band). This is in broad agreement with a visual inspection of the PA waveform which normally indicates a broadband signal with a high amplitude sharp peak time-locked to the pulse, followed by a complex oscillating waveform. PA subtraction reduced this increase in EEG amplitude substantially in all frequency bands, which suggests that the average PA waveform calculated by the method is a good approximation to the true PA waveform. However, there are still some residual components after subtraction—these presumably reflect a small difference between the averaged and the current PA waveforms due to beat-to-beat variations in the PA and the inclusion in the average of non-PA waveforms. These residual components may give rise to spurious signals in the corrected traces. However, the significant reduction in artifact shown by the spectral analysis and the reduction in the number of falsely identified spikes in the EEG corrected by PA subtraction suggest these spurious signals are not a significant problem. Further improvement may be possible by detecting trends in the PA waveform (for example due to respiration) and adjusting the amplitude of the subtraction waveform accordingly. Although more sophisticated methods may reduce further the residual components, we have demonstrated that the method described here has utility in its present form.

The PA subtraction method increased the proportion of lateralized spikes correctly identified in recordings from inside the scanner from 35 to 73% and reduced the rate of false spike detections from 15.7 to 8.7 per hour. This has important benefits for EEG/fMRI studies: as fewer spikes are missed, a rest acquisition is less likely to contain a spike; as there are fewer false detections, an activation acquisition is more likely to contain a spike. Fewer missed spikes also helps to shorten the duration of an EEG/fMRI study which is important as our experience of spike-triggered fMRI studies has indicated that these may last over 1 h. We have only described the effect of PA subtraction on the identification of spikes. For larger amplitude or longer duration events such as electrographic seizures or generalized spike-and-wave, PA subtraction may not be relevant.

Although the evaluation of the PA subtraction method was performed retrospectively, since implementing the method on-line, adequate quality EEG has been obtained in 22/22 EEG/fMRI studies performed—without PA subtraction this would only have been the case in 9/22 studies.

CONCLUSIONS

Pulse artifact is frequently present in EEG recordings in the MR scanner. In five of six subjects in which the full 10/20 system of electrodes was recorded, pulse artifact exceeded 50 μV in at least one of the 13 bipolar derivations analyzed. Large interindividual variations in the amplitude of pulse artifact were observed, and in some subjects it is clear that reliable identification of low amplitude or brief EEG events during an EEG/fMRI study will be extremely difficult. Hence, a method for removing the PA has been developed. We have demonstrated that despite the complexities and beat-to-beat variations of the PA waveform, its subtraction is feasible. This method has been shown to improve the identification of spikes in recordings with large PA. The benefits of this are a greater likelihood of correct triggering of fMRI acquisition and shorter study duration. PA subtraction is likely to become more important as scanners with higher B_0 field strength, and hence greater pulse artifact, come into use.

ACKNOWLEDGMENTS

The authors acknowledge the help given by Michelle Noble and Rachel Jefferys from the Sir Jules Thorn Telemetry Unit, The National Hospital for Neurology and Neurosurgery, London, in reviewing the EEG recordings containing spikes. This study was supported by the National Society for Epilepsy, Chalfont St. Peter, Buckinghamshire, UK, and the Sir Jules Thorn Telemetry Unit, The National Hospital for Neurology and Neurosurgery, Queen Square, London, UK.

REFERENCES

Felblinger, J., Müri, R. M., Rösler, K. M., Jung, B., Hess, C. W., and Boesch, C. 1997. EEG and visually evoked potential recordings in the MR environment. *Proc. Int. Soc. Magn. Res. Med.* **3:**1653.

Hennig, J., Janz, C., Speck, O., and Ernst, T. 1995. Functional spectroscopy of brain activation following a single light pulse: Examinations of the mechanism of fast initial response. *Int. J. Imaging Syst. Technol.* **6**(2/3):203–208.

Hill, R. A., Chiappa, K. H., Huang-Hellinger, F., and Jenkins, B. G. 1995. EEG during MR imaging: Differentiation of movement artifact from paroxysmal cortical activity. *Neurology* **45:**1942–1943.

Huang-Hellinger, F., Breiter, H. C., McCormack, G., Cohen, M. S., Kwong, K. K., Sutton, J. P., Savoy, R. L., Weisskoff, R. M., Davis, T. L., Baker, J. R., Belliveau, J. W., and Rosen, B. R. 1995. Simultaneous functional magnetic resonance imaging and electrophysiological recording. *Hum. Brain Mapp.* **3:**13–23.

Humberstone, M., Sawle, G. V., Clare, S., Hykin, J., Coxon, R., Bowtell, R., Macdonald, I. A., and Morris, P. G. 1997. Functional magnetic resonance imaging of single motor events reveals human presupplementary motor area. *Ann. Neurol.* **42**(4):632–636.

Ives, J. R., Warach, S., Schmitt, F., Edelman, R. R., and Schomer, D. L. 1993. Monitoring the patient's EEG during echo planar MRI. *Electroencephalogr. Clin. Neurophysiol.* **87:**417–420.

Kolin, A. 1952. Improved apparatus and technique for electromagnetic determination of blood flow. *Rev. Sci. Instrum.* **23:**235–242.

Lemieux, L., Allen, P. J., Franconi, F., Symms, M. R., and Fish, D. R. 1997. Recording of EEG during fMRI experiments: Patient safety. *Magn. Res. Med.* **38**(6):943–952.

Patel, P., Al-Dayeh, L., and Singh, M. 1997. Localisation of alpha activity by simultaneous fMRI and EEG measurements. *Proc. Int. Soc. Magn. Res. Med.* **3:**1653.

Tenforde, T. S., Gaffey, C. T., Moyer, B. R., and Budinger, T. F. 1983. Cardiovascular alterations in Macaca monkeys exposed to stationary magnetic fields: Experimental observations and theoretical analysis. *Bioelectromagnetics* **4:**1–9.

Warach, S., Ives, J. R., Schlaug, G., Patel, M. D., Darby, D. G., Thangaraj, V., Edelman, R. R., and Schomer, D. L. 1996. EEG-triggered echo-planar functional MRI in epilepsy. *Neurology* **47:**89–93.

Wendt, R. E., Rokey, R., Vick, G. W., and Johnston, D. L. 1988. Electrocardiographic gating and monitoring in NMR imaging. *Magn. Reson. Imaging* **6:**89–95.